# Design of a Carbon Fiber Rotor in a Dual Rotor Axial Flux Motor for Electric Aircraft


Chase Wiley
*Department of Aerospace Engineering*
*Texas A&M University*
College Station, TX, USA
chase.wiley@tamu.edu

Dorsa Talebi
*Department of Electrical Engineering*
*Texas A&M University*
College Station, TX, USA
dorsa.talebi@tamu.edu

Sri Vignesh Sankarraman
*Department of Electrical Engineering*
*University of Texas at Dallas*
Richardson, TX, USA
SriVignesh.Sankarraman@utdallas.edu

Matthew C. Gardner
*Department of Electrical Engineering*
*University of Texas at Dallas*
Richardson, TX, USA
Matthew.Gardner@utdallas.edu

Moble Benedict
*Department of Aerospace Engineering*
*Texas A&M University*
College Station, TX, USA
benedict@tamu.edu



***Abstract*—Due to the interest in electrifying aviation, a study on the electromagnetic and structural design space of a 250 kW dual rotor axial flux electric motor is presented. For commercial viability, the powertrain must have a high specific power, so the entire motor must be as lightweight as possible. The structural design utilizes carbon fiber reinforced polymers (CFRP), which are extensively being used in the aerospace industry for its high-strength, high-stiffness, and low density. The paper presents three separate structural configurations achieving certain relevant performance criteria for the rotor with increasing complexity, and the mass of these CFRP configurations are compared with each other. By taking advantage of the CFRP's anisotropy and appropriately distributing the CFRP mass, the structural mass can be reduced by 59% relative to a solid disk. Then, the pareto frontiers of the carbon fiber designs will be compared with that of aluminum and titanium structural designs to highlight the mass reduction benefits. The optimal CFRP structure has about half the mass of the optimal aluminum or titanium designs. Finally, a co-optimization study between electromagnetically active components and sufficient structure support is given.**



***Keywords—Electric aviation, carbon fiber, rotor, axial flux, electric motor, decarbonization, optimization***


## I. Introduction

To decarbonize the aviation sectors, the US Advanced Research Projects Agency-Energy (ARPA-E) created the aviation-class synergistically cooled electric motors with integrated drives (ASCEND) program. ASCEND aims to develop a lightweight, highly efficient electric powertrain for commercial aircraft propulsion. ARPA-E determined that for the electric powertrain to be commercially viable for a narrow-body commercial airliner with similar performance to currently operating aircrafts, the system must be at least 93% efficient with ≥12 kW/kg specific power [1], which is a few times higher than state-of-the-art electric motors for aircraft [1]. For this project, an axial flux dual rotor permanent magnet (PM) electric motor is selected [2]. In this dual rotor topology (Fig. 1), grain-oriented electrical steel (GOES), rather than non-oriented electrical steel, can be used to achieve high power density [2] and efficiency [3]. The PM pieces on the rotor are segmented in a Halbach array, which enables the design to replace the rotor back irons with a lightweight nonmagnetic material. However, this lightweight material must also be strong enough to support the axial forces on the rotor.

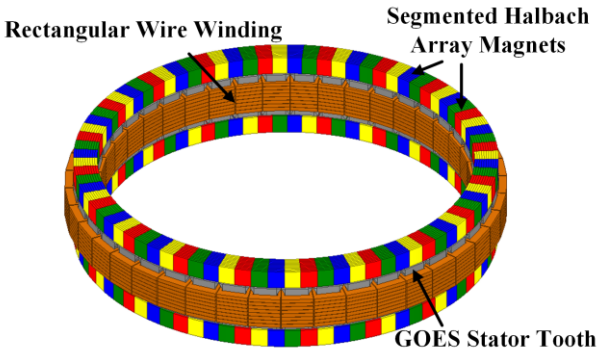


Fig. 1. Electromagnetically active portion of the proposed electric motor

Aluminum, carbon fiber, and titanium are often used in lightweight electric motors. Due to aluminum's low density and high conductivity, aluminum conductors serve as an alternative to copper conductors in lightweight applications [4]. On the other hand, carbon fiber and titanium are much less conductive but have gained traction for wraps/sleeves in traction motor rotors, due to their high strengths [5]. Aluminum's high conductivity limits its use as a structural material in electromagnetically active sections of the motor, as it is prone to eddy current losses. Nonetheless, aluminum can be used as a structural material where there is little variation in the magnetic field, such as in the rotor [6] or the frame of the motor [7]. On the other hand, carbon fiber reinforced polymers (CFRPs) have low conductivity and can be used in both rotor and stator support structures [8] to reduce eddy current losses. In magnetic gears, CFRPs have been used as support material [9]. Titanium has more conductivity than CFRP and, hence, cannot be used as a


This work was supported in part by the U.S. Department of Energy under Award Number DE-AR0001356.

TABLE I. MECHANICAL PROPERTIES OF ALUMINUM, TITANIUM, AND IM7/8552 UNIDIRECTIONAL COMPOSITE

| Material | Density (g/cm$^3$) | Young's Modulus (GPa) | Failure Strength (MPa) | Specific Stiffness (GPa/(g/cm$^3$)) | Specific Strength (MPa/(g/cm$^3$)) |
|---|---|---|---|---|---|
| Aluminum 6061-T6 | 2.71 | 68.3 | 234 | 25.2 | 86.3 |
| Titanium Ti-6Al-4V | 4.43 | 110 | 869 | 24.8 | 196 |
| CFRP:IM7/8552 (Unidirectional) | 1.55 | 171 | 2326 | 110 | 1500 |

support structure as easily as CFRP, but some applications employ titanium alloy as a support material [8], [10].

In aerospace applications, it is often the goal to create structures and key components with minimal mass. Advances in materials science have helped create aircraft with higher performance and more payload capability and, most recently, have enabled entire new industries such as electric aviation. In the past few decades, two classes of metallics have dominated much of the aircraft design - aluminum and titanium. Many alloys of these materials have been created, and more will likely continue to be made to further the state of the art. In this paper, two particular aluminum and titanium alloys, which find extensive use in the aerospace industry, were chosen: aluminum 2024-T3 and Ti-4V-6Al. While these alloys generally do well and represent the performance capabilities of these material classes, there are likely other alloys which may better suit specific applications. Today, CFRPs are replacing many metallic structures in aircraft [11]. Table I lists typical mechanical properties for these materials [12], [13]. As shown in Table I, CFRPs outperform metals, due to their high stiffness, high strengths, and low density. Note that the failure strength values given are based on yield strength for Aluminum, and ultimate strength for Titanium and IM7/8552 since these tend to be brittle. Thus, conventional combustion aircraft engines that are in use today are tending to move towards more weight efficient composite materials as in the case of the Boeing 787 [14]. However, the relatively low maximum service temperature of composites is a key limitation in combustion powertrains since turbine combustion chamber can exceed 1000 °C, but, for the proposed electric motor, the rotor temperatures are not expected to exceed 100 °C. This enables the thorough use of carbon fiber composites in the rotors, facilitating extreme mass reduction, and further highlighting the competitive advantage of electric powertrains over conventional combustion engines in aerospace applications.

In the following sections, initial electromagnetic and mechanical designs are explored. For the mechanical design, designs with carbon fiber polymers are optimized and compared against optimized designs using aluminum or titanium for the rotor structure. Based on the lessons learned from the initial designs, the electromagnetic and structural designs are co-optimized to yield the global optimal design.

## II. ELECTROMAGNETIC DESIGN

Ref. [2] describes the initial electromagnetic design sweep for characterizing the electromagnetic performance in terms of the interfacial parameters with other subsystems, such as the inverter, structure, and thermal management system. Fig. 2 shows the takeoff efficiency (considering only DC copper losses and core losses) and electromagnetically (EM) active mass for the best designs that achieve the required torque (480 Nm). Fig. 2 also shows the axial forces that the rotor structure must

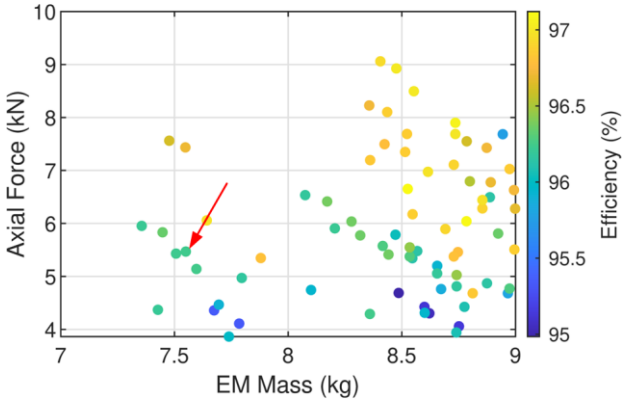


Fig. 2. Axial rotor force, electromagnetically active mass, and takeoff electromagnetic efficiency of the best points in the electromagnetic design sweep

TABLE II. MECHANICAL PROPERTIES OF ALUMINUM, TITANIUM, AND IM7/8552 UNIDIRECTIONAL COMPOSITE

| Parameter | Values |
|---|---|
| Peak takeoff power (kW) | 250 |
| Cruise power (kW) | 83 |
| Takeoff speed (RPM) | 5000 |
| Cruise speed (RPM) | 4000 |
| Pole pairs | 20 |
| Number of stator teeth | 42 |
| Rotor magnet outer diameter (cm) | 27 |
| Rotor magnet inner diameter (cm) | 22 |
| Magnet thickness | 1 |

support. In [2], the axial force was strongly correlated to the magnet thickness and the airgap surface area. Based on the results of the initial electromagnetic analysis, the indicated point in Fig. 2 was selected as a baseline for the structural design. Fig. 1 illustrates the electromagnetically active portions of the selected baseline design, and Table II summarizes the motor design parameters.

## III. STRUCTURAL DESIGN WITH CARBON FIBER COMPOSITES

Unlike metals, CFRP is anisotropic, which means that its material properties vary depending on the orientation of fibers. Fig. 3 shows the direction-1 runs parallel to the fibers and direction-2 runs perpendicular to the fibers. The mechanical properties with respect to these two directions are the elastic Young's moduli E1, E2, the shear modulus G12, and the Poisson ratio ν12. E1 is typically much higher than E2, and an example of properties for the IM7/8552 composite can be seen in Table III [13]. Comparing these values with those of the isotropic aluminum and titanium alloys shows a fundamental difference in how the materials behave and opens up many new design possibilities in achieving the required structural performance.

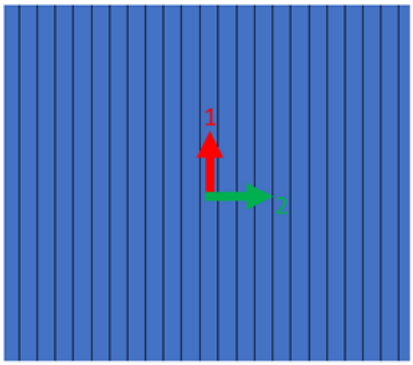


Fig. 3: Composite plate with material axes shown. 1 runs parallel to the fibers, 2 runs transverse to the fibers.

Due to the large attractive forces between the rotor magnets and the stator, the rotor structure for this electromagnetic configuration must support a strong distributed axial force. At a nominal one-side air gap distance of 1.25 mm, a total magnitude of 5.75 kN acts on the magnets and rotor structure as shown in Fig. 4. For an axial flux motor, the resulting rotor structure deflections reduce the airgap and further increase the axial forces, as these forces are inversely related to distance. A functional rotor structure design must be stiff enough that a maximum deflection is not exceeded; otherwise, the air gap could close entirely and cause a catastrophic failure during operation. Because the load is out of the plane, the structure undergoes bending and careful attention must be paid to ensure the structure deflects minimally and evenly along the outer circumference.

When designing any component, certain constraints are given (geometric, performance, etc.), which the structure needs to satisfy. Furthermore, in the design of lightweight components, the structure not only needs to satisfy constraints but also be competitive with mass. In the field of optimization, this is typically referred to as the cost function, and it is sought to minimize this value. To find the best possible design (which minimizes the cost function), an optimization algorithm is typically used. A genetic algorithm script created in the Python language was employed with finite element analysis (FEA) in ABAQUS to find the minimum mass designs that satisfy a given deflection constraint. In this case, the rotor structures are not allowed to deflect more than 0.3 mm.

In designing structures with metallics, once a material is chosen upon, the design variables are typically only geometrical. However, with CFRPs, even after a material is chosen it is not enough to consider only geometric variables in the design space. One must also consider the laminate stacking sequence, as well.

TABLE III: IM7/8552 MECHANICAL PROPERTIES

| | |
|---|---|
| **Density (g/cc)** | 1.55 |
| **E1 (GPa)** | 171.4 |
| **E2 (GPa)** | 9.08 |
| **G12 (GPa)** | 5.29 |
| **v12** | 0.32 |
| **v23** | 0.4 |

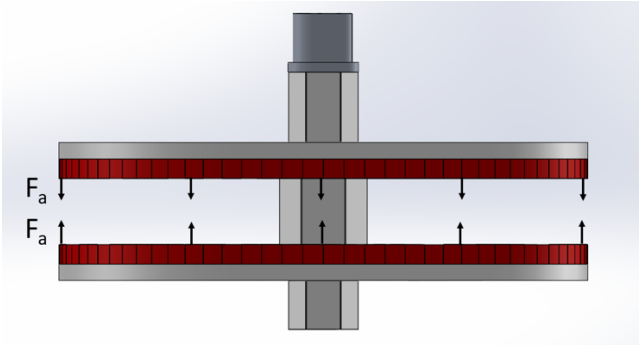


Fig. 4. Electromagnetic axial load on rotor structures

The laminate stacking sequence dictates how the plies should be oriented and in what order. For example, a sequence of [0,45,90] would consist of 3 plies stacked with fiber orientations of 0°, then 45°, then 90° relative to a reference axis. The choice of laminate stacking sequence has a direct and strong impact on the performance of the structure, as this affects the structure's mechanical properties. A quasi-isotropic symmetric laminate stacking sequence ensures in-plane mechanical properties (E1, G12, etc.) are constant in all planar directions. The initial and most basic choice of structure would be a solid disk consisting of a quasi-isotropic layup. Fig. 5 shows the plot of overall mass vs maximum deflection experienced for the solid disk structure with varying thickness, based on ABAQUS FEA. To maintain a deflection no larger than 0.3 mm, the optimal solid quasi-isotropic disk requires 1000 g.

Once the baseline deflection and optimal mass of the solid disk structure is obtained, mass can be strategically relocated to increase the bending inertia. An example of this process is by "cutting out" 8 spokes of material and re-applying that mass as added thickness to the design as seen in Fig. 6. This results in a stiffer structure for the same mass. Since composite structures benefit the most from continuous fibers, it is useful to employ a laminate stacking sequence which contains plies that only run in the direction of a spoke, hence $[0,90,45,-45]_{4,S}$ in this case. Weight optimal components were then obtained using a genetic algorithm optimization script coupled with ABAQUS FEA. For a deflection of 0.3 mm, the best possible mass obtained was 941 grams with this structure, which is 6% lighter than the solid disk with the same deflection.

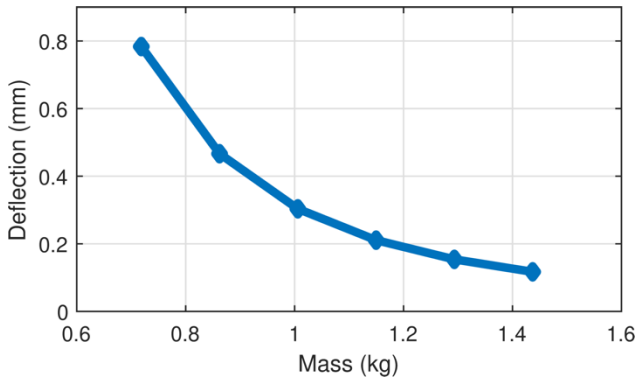


Fig. 5. Solid disk mass vs deflection

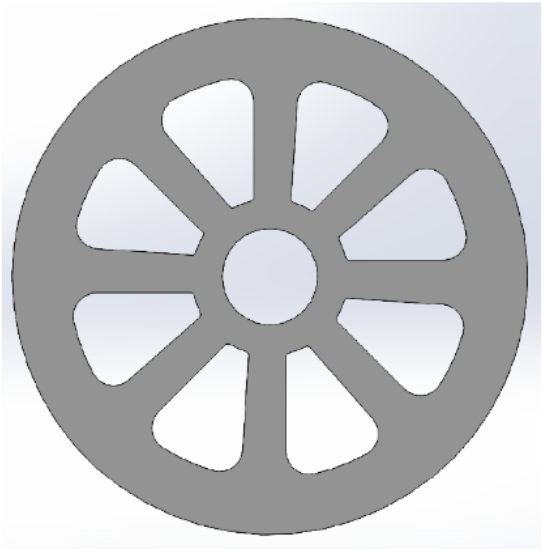

Fig. 6. Example of the spoke shaped cutouts on the rotor disk structure

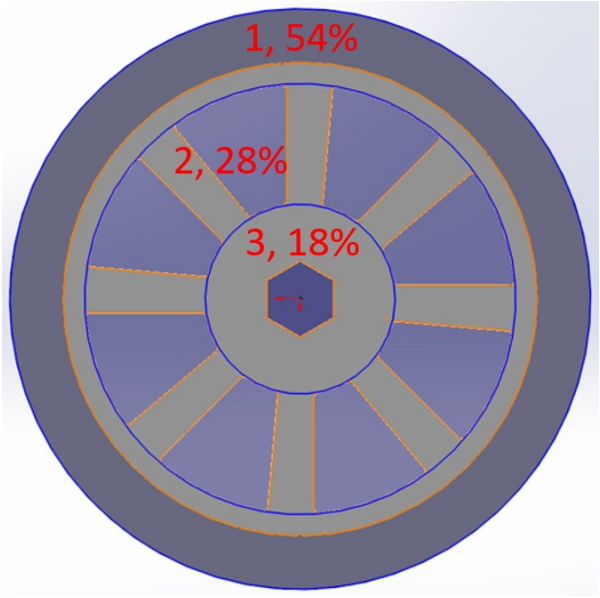


Fig. 7. Rotor disk decomposition with mass percentage for each section

A quasi-isotropic structure fails to take advantage of the anisotropy of CFRPs. Fig. 7 shows the structure given in Fig. 6 decomposed into three main sections with their corresponding mass percentage: 1) the magnet mounting disk, 2) the spokes, and 3) the root. The magnet mounting disk simply holds the magnets, the spokes transfer the load to the root, and the root transfers loads to the shaft while providing a stable root condition. The magnet mounting disk has the largest area and accounts for most of the mass, despite least affecting the overall structural deflections due to being the furthest from the root. Therefore, the previous quasi-isotropic rotor disk portion of the design was discarded in favor of an assembly with 3 unique components as seen in Fig. 8. This allows parts which minimally affect the overall deflection reduction to have low mass while also introducing unidirectional box beams along the spokes to

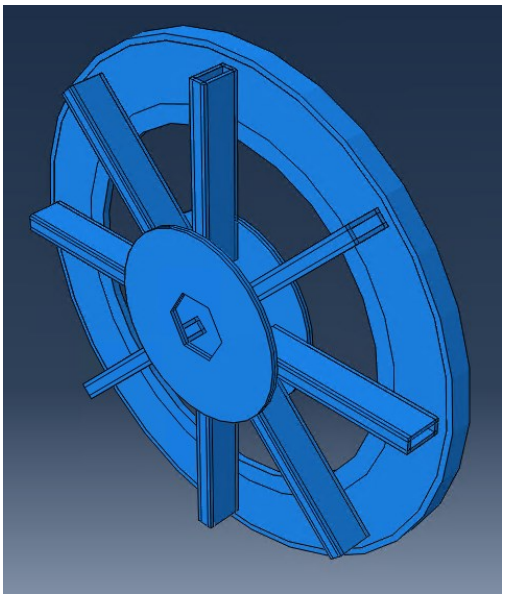

Fig. 8. Rotor disk design with unidirectional box spokes

maximize bending stiffness. For a structure with the same deflection as the original 941 g quasi-isotropic disk, this new configuration yields a 406 g structure after optimization.

## IV. Optimal Structural Design with Metallics and Comparisons

Using the same methodology in determining the optimal composite structure, optimal aluminum and titanium rotor structures are found using the mechanical properties given in Table I. One critical thing to note is that while static structural studies are being performed to determine axial deflections in finding the best design, it is important to remember that this structure will undergo rotations and, thus, will apply a large centripetal force to the magnets. To sufficiently support these forces, a minimum sizing of the retaining ring wall thickness is needed depending on the material used. Given that a failure of the retaining ring will result in catastrophic destruction of the motor, a large safety factor was applied to the material strengths given in Table I and are identified in Table IV. A value of 3 was applied to Aluminum's yield strength, while 4 was applied to Titanium and IM7/8552's ultimate strength. With a given design rotation of 5000 RPM, the corresponding magnet masses of 1443 grams per rotor, and conservatively using the radial distance from the center of rotation to the furthest point of the magnets at 135 mm, an estimate of the total centripetal force experienced is 53.5 kN. By dividing this value by the outer circumference, the edge loading is 63 kN/m. If this loading is treated as applying an internal pressure to a thin ring, then the hoop stress can be found and used to help determine the minimum thickness necessary for the retaining ring. The

TABLE IV: Retaining Ring Sizing by Material

| Material | Strength Safety Factor | Design Strength (MPa) | Minimum Thickness (mm) |
|---|---|---|---|
| Al 2024-T3 | 3 | 75 | 11.34 |
| Ti-6Al-4V | 4 | 195 | 4.36 |
| IM7/8552 | 4 | 582 | 1.46 |

pressure is found by distributing the edge load across the height of the magnets, in this case 10 mm, which computes to a pressure of 6.3 MPa. Calculating the minimum ring thickness using the formula for hoop stress yields the values are tabulated in Table IV. These retaining ring thickness values were enforced on each optimization study as a minimum design variable bound. Note that in the case of the composite, this is the minimum thickness of unidirectional plies needed. A good composite design would also incorporate about 25% of off-axis plies, so in this study analysis was performed with a minimum 2mm thick retaining ring composed of 1.5 mm of unidirectional and 0.5mm of off-axis plies. Additionally, the same optimization study was performed on a "hybrid" design which used an aluminum rotor structure with a CFRP retaining ring. The generated pareto frontiers are given in Fig. 9. For a performance target of 0.3 mm axial deflection, the following optimal masses are given in Table V.

TABLE V: OPTIMAL STRUCTURE MASS BY MATERIAL

| Material | Optimal Mass (g) |
|---|---|
| IM7/8552 | 406 |
| Al 2024-T3 | 831 |
| Ti-6Al-4V | 819 |
| Hybrid | 600 |

## V. ELECTROMAGNETIC AND STRUCTURAL CO-OPTIMIZATION

Performing a new set of electromagnetic parametric sweep studies introduces lighter active material designs with higher efficiency (accounting all the DC and AC losses in the active material). The new studies basically involved small perturbations of the design parameters around the initial baseline design. Fig. 10 shows the efficiency, total active mass, and no load rotor axial force of the best 21 designs resulting from this study and the baseline design selected from the previous study. Some of these designs have a larger outer diameter with a shorter stack which results in a higher torque per amp coefficient due to a larger torque arm. The parameters of the rotor PMs for these new cases can be divided into the configurations listed in Table VI; these dimensional parameters, together with the axial force on the rotor are key parameters that determine the mass of the rotor structure. Thus, further analysis of the new designs regarding the structural system is crucial since increasing the outer diameter or the axial force increases the structural mass, as shown in Fig 11. Configuration 1, which has the smallest outer

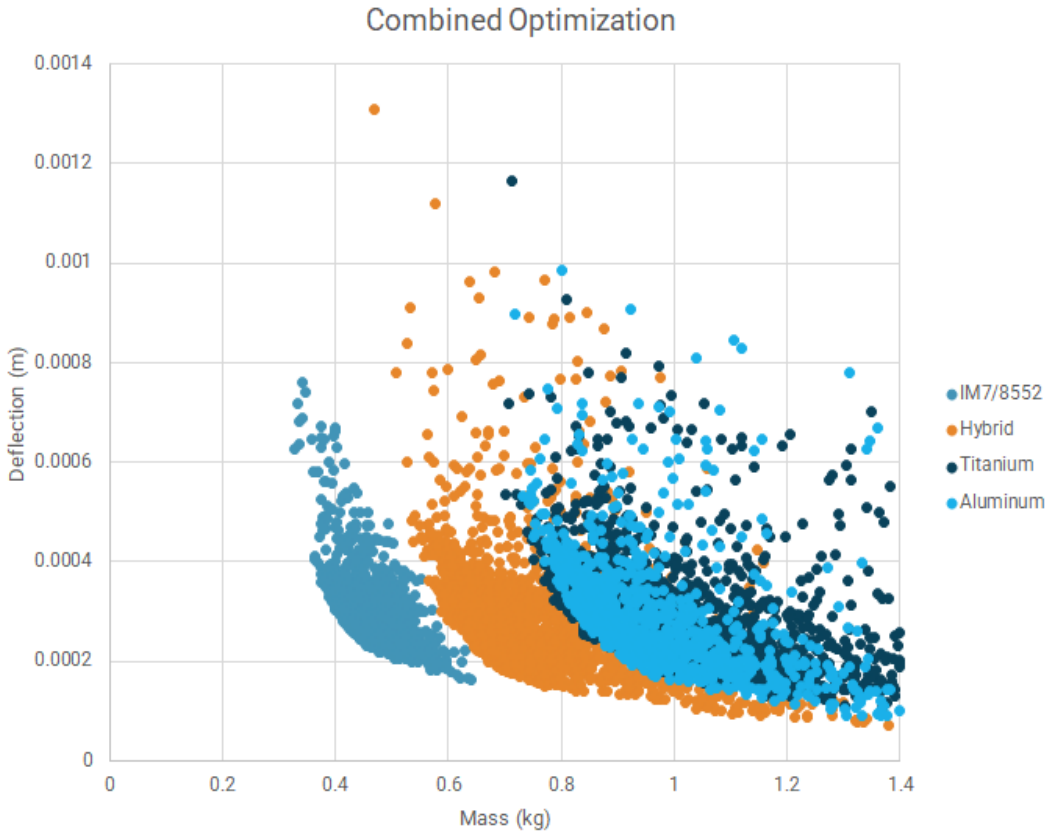


Fig. 9. Pareto frontiers of rotor structure masses vs deflections for 4 material choices

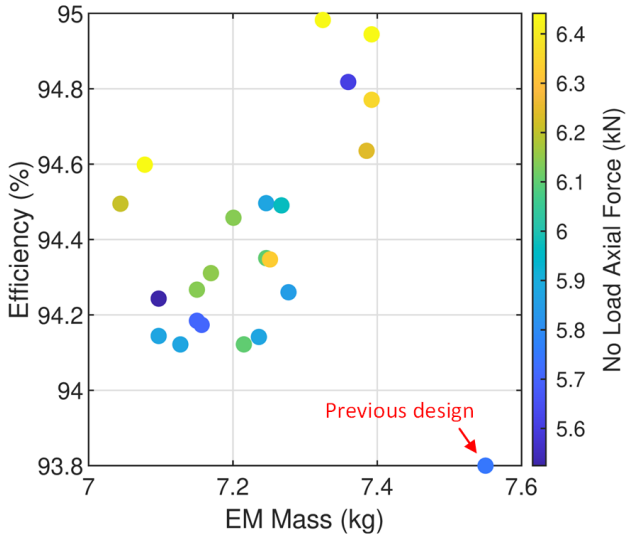


Fig. 10. Efficiency, total active mass, and no load axial force for new electromagnetic configuration sweep

TABLE VI: ELECTROMAGNETIC CONFIGURATION PARAMETERS

| Configuration | Magnet Inner Radius (mm) | Magnet Outer Radius (mm) | Magnet Length (mm) |
|---|---|---|---|
| Original | 110 | 135 | 10 |
| 1 | 105 | 135 | 8 |
| 2 | 110 | 140 | 8 |
| 3 | 115 | 140 | 10 |

diameter considered, shows a clear advantage for minimizing structural mass.

Combining these structural masses with that of the active electromagnetic masses and plotting against axial force experienced gives Fig. 12. Fig. 13 compares the total mass between each design in bar chart format. Fig. 14 provides the total mass, together with the efficiency and no-load axial force.

## VI. CONCLUSIONS

This paper provides design of CFRP rotor structure support for an axial flux dual rotor electric motor configuration aiming an extreme lightweight powertrain system in aviation application. As a starting point, the optimal electromagnetic design from [2] is used and summarized in Table II. Using IM7/8552 carbon fiber composite, three different structural designs are mass optimized to prevent over 0.3mm of deflection under a 5.75 kN axial force. The first, a solid disk with a quasi-isotropic layup yielded a 1000 g design. Using a spoked design, as given in Fig. 6, with a quasi-isotropic layup reduces the mass to 941 g. However, when using box beam spokes with a unidirectional layup to leverage the anisotropy of the CFRP like the design in Fig. 8, the optimal mass found is 406 g, which is a 57% weight reduction. When applying the same optimization method to structures of Aluminum 2024-T3, Titanium 4V-6Al, and a hybrid with an aluminum structure and a carbon fiber retaining ring, optimal masses of 831, 819, and 600 grams are found, respectively. Thus, CFRPs can yield a significant reduction in structural mass relative to metallics. However, this benefit is only realized if the structural design takes advantage of CFRP's anisotropic properties.

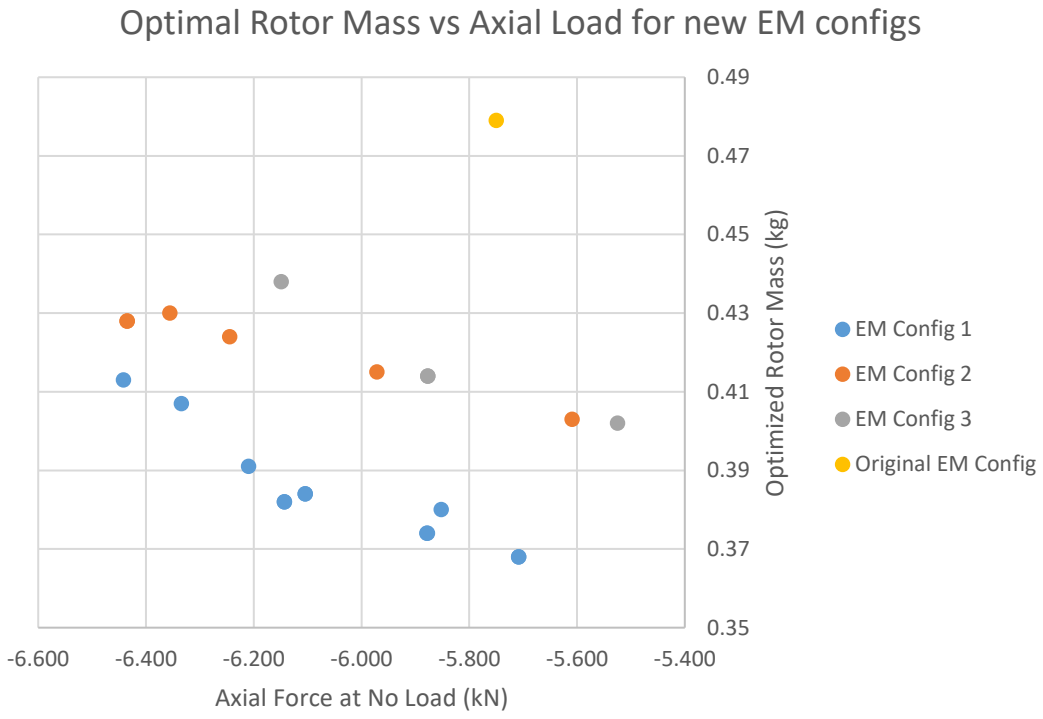


Fig. 11. Mass optimal composite rotor structure masses vs axial load for new electromagnetic configurations

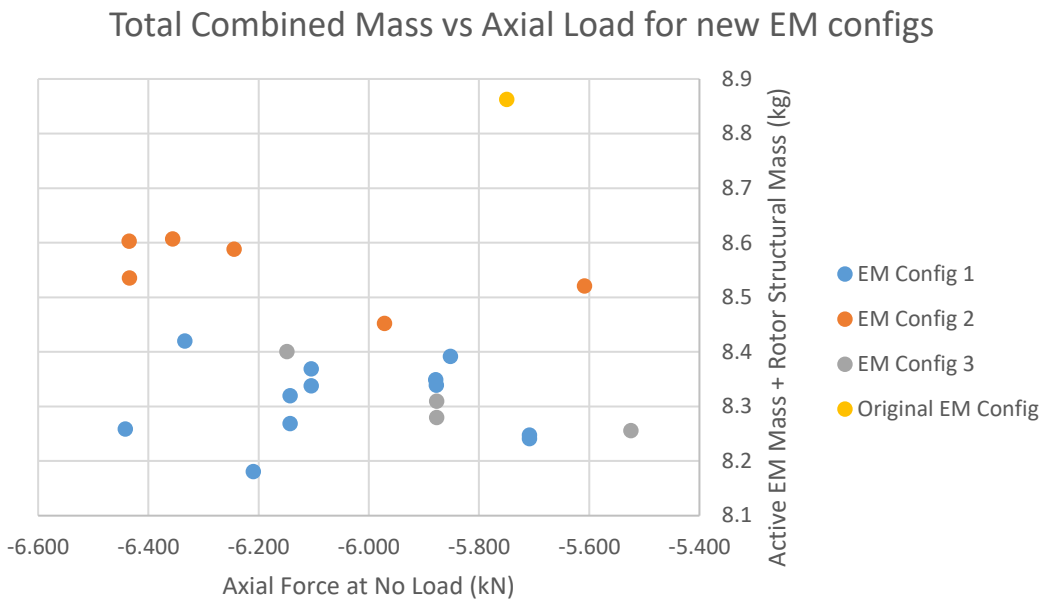


Fig. 12. Combined electromagnetic and rotor structural masses vs axial forces for new electromagnetic configurations

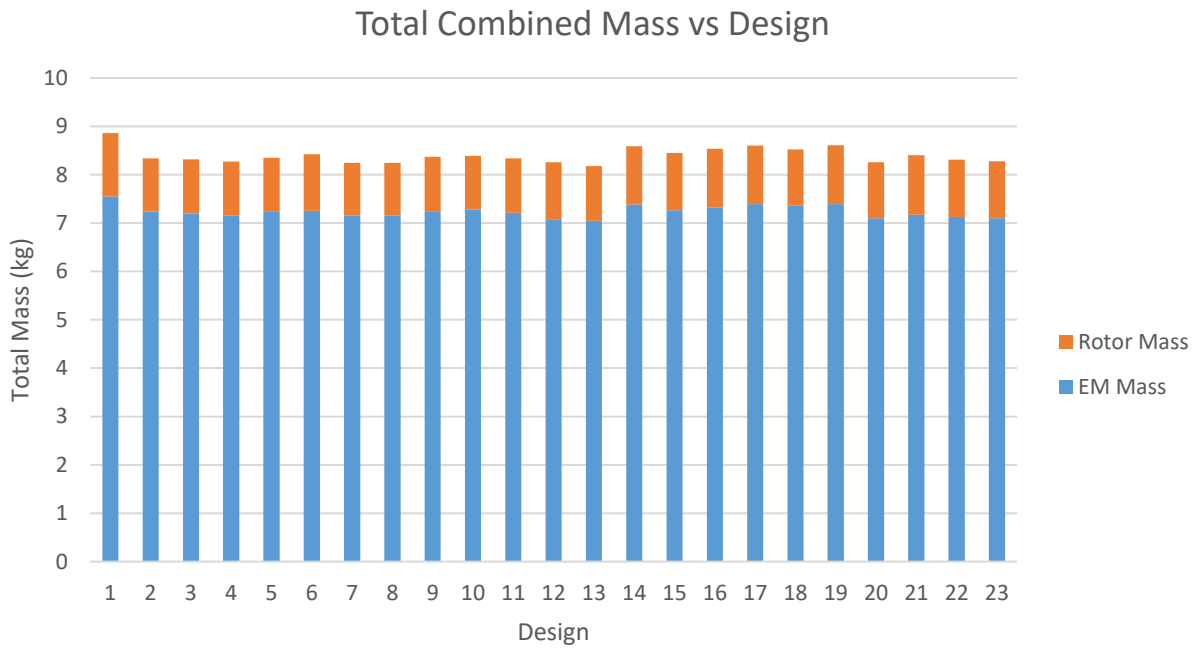


Fig. 13. Bar graph showing combined electromagnetic and structural masses for each new configuration examined. Design 1 is the original design.

A new parametric sweep of the electromagnetic design was performed, with 22 new design points generated and characterized in Fig. 10. From this, the same optimization method was performed using IM7/8552 CFRP on each new configuration, with results given in Figs. 11-14. A clear trend between increasing axial force and optimal mass is given in Fig. 11, when only considering rotor structure. However, when electromagnetic masses are added, no such clear trend emerges as seen in Fig. 12. Fig. 13 summarizes the combined optimal mass results, which shows an overall optimal mass configuration of 8.181 kg including the motor with the EM active material and the rotor structure. This is a reduction of 682 grams from the original 8.863 kg configuration.

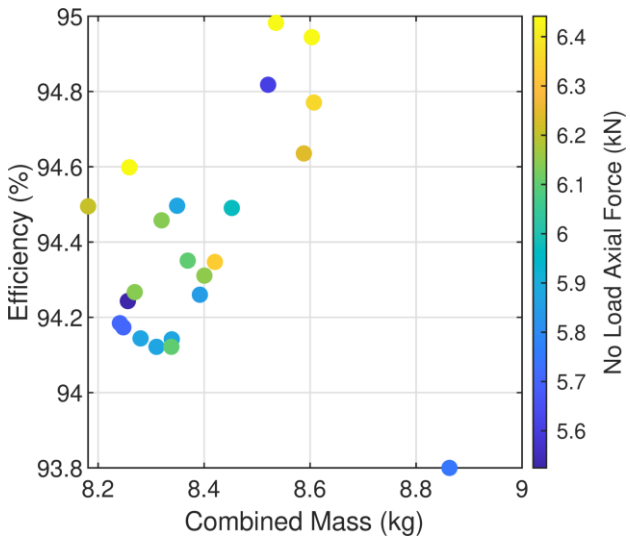


Fig. 14. Combined structural and electromagnetic masses for the new electromagnetic parameter sweep

## ACKNOWLEDGMENT

Portions of this research were conducted with the advanced computing resources provided by Texas A&M High Performance Research Computing. The authors would like to thank ANSYS for their support of the EMPE lab through the provision of FEA software.

This material is based upon work supported by the Department of Energy under Award Number DE-AR0001356. This report was prepared as an account of work sponsored by an agency of the United States Government. Neither the United States Government nor any agency thereof, nor any of their employees, makes any warranty, express or implied, or assumes any legal liability or responsibility for the accuracy, completeness, or usefulness of any information, apparatus, product, or process disclosed, or represents that its use would not infringe privately owned rights. Reference herein to any specific commercial product, process, or service by trade name, trademark, manufacturer, or otherwise does not necessarily constitute or imply its endorsement, recommendation, or favoring by the United States Government or any agency thereof. The views and opinions of authors expressed herein do not necessarily state or reflect those of the United States Government or any agency thereof.

## REFERENCES

[1] "DE-FOA-0002238: Aviation-class synergistically cooled electric-motors with integrated drives (ASCEND)", Department of Energy, Advanced Research Projects Agency Energy, Dec. 2019.

[2] D. Talebi, M. C. Gardner, S. V. Sankarraman, A. Daniar, and H. A. Toliyat, "Electromagnetic Design Characterization of a Dual Rotor Axial Flux Motor for Electric Aircraft," in *Proc. IEEE Int. Elect. Mach. and Drives Conf.*, 2021, pp. 1-8.

[3] M. C. Gardner, Y. Zhang, D. Talebi, H. A. Toliyat, A. Crapo, P. Knauer, and H. Willis, "Loss Breakdown of a Dual Conical Rotor Permanent Magnet Motor using Grain Oriented Electrical Steel and Soft Magnetic Composites," in *Proc. IEEE Int. Elect. Mach. and Drives Conf.*, 2019, pp 1067-1074.

[4] J. D. Widmer, C. M. Spargo, G. J. Atkinson, and B. C. Mecrow, "Solar Plane Propulsion Motors With Precompressed Aluminum Stator Windings," *IEEE Trans. Energy Convers.*, vol. 29, no. 3, pp. 681-688, Sept. 2014.

[5] K. Grace, S. Galioto, K. Bodla and A. M. El-Refaie, "Design and Testing of a Carbon-Fiber-Wrapped Synchronous Reluctance Traction Motor," *IEEE Trans. Ind. Appl.*, vol. 54, no. 5, pp. 4207-4217, Sept.-Oct. 2018.

[6] J. Oyama, T. Higuchi, T. Abe and K. Tanaka, "The fundamental characteristics of novel switched reluctance motor with segment core embedded in aluminum rotor block," in *Proc. Int. Conf. Elect. Mach. Syst.*, 2005, pp. 515-519.

[7] Regal Beloit, "Marathon Motors Catalog", 2018.

[8] Y. Wei, J. Bai, B. Yu, Z. Yin and P. Zheng, "Mover Optimization and Mechanical Strength Analysis of a Tubular Permanent-Magnet Linear Motor," in *Proc. Int. Conf. Elect. Mach. Syst*, 2019, pp. 1-4.

[9] T. F. Tallerico, Z. A. Cameron and J. J. Scheidler, "Design of a Magnetic Gear for NASA's Vertical Lift Quadrotor Concept Vehicle," in *Proc. AIAA/IEEE Elect. Aircraft Technol. Symp.*, 2019, pp. 1-21.

[10] Y. Yu et al., "Rotordynamic Assessment for an Inside Out, High Speed Permanent Magnet Synchronous Motor," in *Proc. Int. Conf. Elect. Mach.*, 2020, pp. 529-535.

[11] G. Marsh, Airframers exploit composites in battle for supremacy, *Reinforced Plastics*, vol. 49, no. 3, pp. 26-32, 2005.

[12] MMPDS-11: Metallic Materials Properties Development and Standardization (MMPDS). Federal Aviation Administration, 2016.

[13] E. J. Barbaro, *Introduction to Composite Materials Design*, Taylor & Fancis Group, 2017.

[14] S. F. Clark, "787 Propulsion System." *Boeing Aero Magazine*, Boeing, 2012.